Multisensory integration enhances audiovisual responses in the Mauthner cell

Santiago Otero-Coronel[1], Thomas Preuss[2] and Violeta Medan[1,3]*

Abbreviated title: Multisensory integration in the Mauthner cell

1. Instituto de Fisiología y Biología Molecular y Celular, Concejo Nacional de Investigaciones Científicas y Tecnológicas, Buenos Aires, Argentina (1428).
2. Dept. Psychology, Hunter College, City University of New York, New York, NY, USA (10065).
3. Dept. Fisiología y Biología Molecular y Celular, Facultad de Ciencias Exactas y Naturales, Universidad de Buenos Aires, Buenos Aires, Argentina (1428).

*Corresponding author, e-mail: violetamedan@fbmc.fcen.uba.ar.

Number of pages: 22
Number of figures: 6
Number of words: Abstract 194, Introduction 615, Discussion 1316.
Conflict of interest statement: The authors declare no competing financial interests.

ACKNOWLEDGEMENTS

This work was supported by PICT 2012-1578 and PICT 2017-0007, FONCYT-ANPCYT (VM), PIP 11220130100729CO (VM), UBACyT 20020130300008BA (VM), Thalmann Program, University of Buenos Aires (VM) SOC was supported by undergraduate fellowships from the National Interuniversity Council and University of Buenos Aires. The authors thank Dr. Lidia Szczupak and members of the Medan lab for discussion and for reading previous versions of this manuscript. Current address of SOC is at The Rockefeller University, New York, NY, USA (10065).

ABSTRACT

Multisensory integration combines information from multiple sensory modalities to create a coherent perception of the world. In contexts where sensory information is limited or equivocal, it also allows animals to integrate individually ambiguous stimuli into a clearer or more accurate percept and, thus, react with a more adaptive behavioral response. Although responses to multisensory stimuli have been described at the neuronal and behavioral levels, a causal or direct link between these two is still missing. In this study, we studied the integration of audiovisual inputs in the Mauthner cell, a command neuron necessary and sufficient to trigger a stereotypical escape response in fish. We performed intracellular recordings while presenting a diverse range of stimuli to determine which stimulus properties affect their integration. Our results show that stimulus modality, intensity, temporal structure, and interstimulus delay affect input summation. Mechanistically, we found that the distinct decay dynamics of feedforward inhibition triggered by auditory and visual stimuli can account for certain aspects of input integration. Altogether, this is the first study to investigate multisensory integration in a cell of clear behavioral relevance and provides a phenomenological and mechanistic characterization of how multisensory integration depends on stimulus properties.

SIGNIFICANCE STATEMENT

In real-world scenarios where sensory information can be ambiguous, mechanisms that reduce the uncertainty and increase information about potential threats is of critical importance. During multisensory integration, independent signals from an event are combined to form a percept with enhanced information. The Mauthner cell is a paramount example of an identified brainstem neural circuit in fish that decides whether or not to execute a fast escape, directly contributing to the animal survival. Here we show that the *mechanistic implementation of multisensory integration at a single-cell level in* the Mauthner cell results from properties of the sensory inputs, restrictions imposed by intrinsic properties, neuronal architecture and network inhibitory effects. Importantly, this multisensory response enhancement has direct and unequivocal impact in animal behavior and survival.

INTRODUCTION

The ability to detect a potential threat and react with a startle/escape behavior is critical for survival. However, escapes are metabolically costly and disruptive of other behaviors, therefore tightly controlled by neural networks that only trigger a response when danger is almost certain. Higher activation thresholds in these neural circuits can reduce the rate of false alarms, requiring clear and salient sensory inputs to trigger a behavioral response. In nature, however, many predators develop strategies such as camouflage or partial hiding to decrease their salience, and sensory stimuli tend to be noisy and ambiguous. Consequently, it is adaptive for animals to have ways to disambiguate the signals from the sensory inflow they receive, especially in contexts where available information is limited.

One strategy for reducing sensory uncertainty is multisensory integration (MSI), which is defined as the process of combining information coming from independent sensory streams to form a new percept with reduced ambiguity (Stein and Stanford, 2008). MSI has been extensively documented in animals from nematodes to humans and in a broad range of behavioral contexts. In the context of escape behaviors, MSI of threat-like stimuli increases the escape probability and reduces the latency of the evoked response. In mammals, activation of different parts of the superior colliculus determines whether animals engage in exploratory or defensive behaviors (Dean et al., 1989; Wei et al., 2015). Importantly, the superior colliculus contains neurons that integrate multisensory stimuli due to synaptic convergence of afferents conveying information from different sensory modalities (Kadunce et al., 2001). These studies established that the effects of MSI are larger when weak or ambiguous stimuli are combined, determining an inverse effectiveness relationship with stimulus strength. The underlying hypothesis is that integration of sensory signals from different modalities form a more accurate world percept only if each unisensory signal carry some uncertainty or ambiguity.

In goldfish, audiovisual MSI increases the probability and reduces the latency of startle escape behaviors, with an inverse relationship between the MSI effectiveness and the stimulus salience (McIntyre and Preuss, 2019; Martorell and Medan, 2022). These startle escapes (C-starts) are triggered by a pair of reticulospinal neurons (Mauthner cells) that receive visual and auditory inputs through anatomically segregated pathways. Auditory inputs reach the M-cell lateral dendrite through a disynaptic (2 ms) pathway, while the visual inputs relay information in the optic tectum before reaching the M-cell ventral dendrite through a polysynaptic (20 ms) pathway (Zottoli et al., 1987; Korn and Faber, 2005; Szabo et al., 2007). The accessibility of M-cells for *in vivo* intracellular recordings and that fact that there is one-to-one relationship between a single M-cell action potential and the initiation of a C-start is well suited to investigate the cellular mechanisms of multisensory integration

with a clear functional consequence (Zottoli, 1977; Weiss et al., 2006). We recently showed that cable properties differ between the auditory and visual M-cell dendrites, putatively to accommodate the different temporal dynamics, excitatory-inhibitory balances, and relative strengths of the respective inputs (Medan et al., 2017). However, it is unclear how auditory and visual signals are integrated at the level of the M-cell to generate a multisensory response. Here we study how visual and auditory presynaptic pathways and intrinsic characteristics of an identified multisensory neuron interact to produce MSI to ultimately enhance threat detection. To this aim we performed somatic intracellular recordings of goldfish M-cell *in vivo* using auditory and tectal stimuli with naturalistic dynamics. Our results show how the temporal dynamics, stimulus strength and feed-forward inhibition affect MSI and reveals an inverse effectiveness relationship between MSI integration and stimulus intensity. This represents a rare characterization of MSI at a single-cell level in a neuron that is sufficient and necessary to trigger a stereotyped behavior.

METHODS

Animals

We used adult goldfish (*Carassius auratus*) of both sexes and 7–10 cm of standard body length. Fish were purchased from Billy Bland Fishery (Taylor, AR, USA), Hunting Creek Fisheries (Thurmont, MD, USA) or Daniel Corriarello Aquarium (Buenos Aires, Argentina) and allowed to acclimate for at least a week after transport. Fish were kept in rectangular Plexiglas holding tanks (30 x 60 x 30 cm^3; 54 l) in groups of up to 10 individuals. Tanks were supplied with filtered and dechlorinated water and maintained at 18 °C. Ambient light was set to a 12-h light/dark photoperiod. Animals were fed floating pellets (Sera, Germany) five times a week. All procedures and protocols were performed in accordance with the guidelines and regulations of the Institutional Animal Care and Use Committee of Hunter College, City University of New York and Facultad de Ciencias Exactas y Naturales, Universidad de Buenos Aires.

Acoustic stimuli

Sound stimuli consisted in single-cycle sound pips (5-ms duration at 200 Hz) produced by a function generator (33210A Agilent Technologies Inc., Santa Clara, CA, USA) connected to a shielded subwoofer (SA-WN250 Sony Corp., Tokyo, Japan) located at 30 cm from the recording chamber. Sound stimuli were recorded with a microphone positioned 10 cm over the head of the fish. For calibration, a hydrophone (SQ01, Sensor Technology, Ontario, Canada) was positioned where the submerged fish was placed during experiments. As a result of transfer loss through the media of the recording chamber (air to water), the maximum underwater sound intensity was 147 dB SPL relative (re) to 1 μPa in water. We deliberately used sound intensities which are known to be subthreshold for evoking behavioral startle responses (Neumeister et al., 2008) as we were interested on studying integration of subthreshold stimuli.

Optic tectum stimulation

Tectal stimuli consisted in the electrical stimulation of the mid-anterior rim of the left optic tectum using a bipolar electrode (#30202 FHC, Bowdoin, ME, USA) connected to an isolated stimulator (DS2A; Digitimer Ltd, Welwyn Garden City, UK). In most cases, stimulation [100 µs, 0.1-1mA] in this area was effective in driving significant responses (> 4 mV) in the M-cell and we did not change the position of the electrode or the amplitude of the current during the experiment. To change the strength and dynamics of the tectal stimulation we either used a 60-Hz stimulation of variable duration (1, 33, 66, 100, 200 ms) or a 100-ms train of variable frequency (1, 33, 100, 200 Hz).

140 **Electrophysiology**

141 Intracellular responses of the M-cell to tectal and acoustic stimuli were studied *in vivo* using standard
142 surgical and electrophysiological recording techniques (Preuss and Faber, 2003; Preuss et al., 2006;
143 Medan et al., 2017). To initiate anesthesia, fish were immersed in 1 liter of ice water with 40 mg/l of
144 the general anesthetic tricaine methanesulfonate (MS-222, Western Chemical, Ferndale, WA, USA),
145 until the fish ceased to swim, lost equilibrium and were unresponsive to a pinch on the tail (typically
146 10–15 min). They were next treated with 20% benzocaine gel (Ultradent, South Jordan, UT, USA) at
147 incision sites and pin-holding points 5 min prior to surgical procedures. Fish were stabilized in the
148 recording chamber by two pins, one on each side of the head, and ventilated through the mouth with
149 recirculating, aerated saline at 18°C (saline [g/l]: sodium chloride 7.25, potassium chloride 0.38,
150 monosodium phosphate monobasic 0.39, magnesium sulphate 0.11, Hepes 4.77; calcium chloride
151 0.24; dextrose 1.01, pH 7.2). The recording chamber was mounted inside an opaque, thin-walled tank
152 filled with saline that covered the fish up to eye level. The recirculating saline also included a
153 maintenance concentration of the anesthetic MS-222 (20 g/l) that does not interfere with auditory
154 processing (Palmer and Mensinger, 2004; Cordova and Braun, 2007). Next, the spinal cord was
155 exposed with a small lateral incision at the caudal midbody. Bipolar stimulation electrodes were placed
156 on the unopened spinal cord to transmit low-intensity (5–8 V) electrical pulses generated by an
157 isolated stimulator (A 360, WPI, Sarasota, FL, USA). This allowed antidromic activation of the M-cell
158 axons, as confirmed by a visible muscular contraction (twitch). Surgical procedures were performed
159 before a muscle paralysis agent was injected, which allows monitoring of the effectiveness the
160 anesthetic by watching for an increase of opercula movement frequency (largely reduced in deep
161 anesthesia) and movements/twitches in response to the surgical procedures. Shortly before the
162 recordings started, animals were injected I.M. with D-tubocurarine (1 μg g−1 b.w.; Abbott
163 Laboratories, Abbott Park, IL, USA) and a small craniotomy exposed the medulla for
164 electrophysiological recordings. Antidromic stimulation produces a negative potential in the M-cell
165 axon cap (typically 15–20 mV), which unambiguously identifies the axon hillock and allows intracellular
166 recordings from defined locations along the M-cell soma-dendritic membrane (Furshpan and
167 Furukawa, 1962; Furukawa, 1966; Faber and Korn, 1989). Intracellular recordings were acquired using
168 borosilicate glass electrodes (7–10 MΩ) filled with 5 M potassium acetate and an Axoclamp-2B
169 amplifier (Axon Instruments, Foster City, CA, USA) in current-clamp setting. M-cell responses were
170 acquired with a Digidata 1440A (Axon Instruments) at 25 kHz. Electrodes were advanced using
171 motorized micromanipulators (MP-285; Sutter Instruments, Novato, CA, USA) until reaching the axon
172 cap (defined as a site with an extracellular M-cell AP field >10 mV). Next, the electrode was moved 50

173 μm lateral and 50 μm posterior to penetrate the somatic region. Only trials in which the resting
174 membrane potential was between -90 and -70 mV were included in the analysis.
175
176 **Experimental Design and Statistical Analyses**
177 Postsynaptic responses to acoustic and tectal or visual stimuli were recorded at the M-cell soma and
178 averages of 5-10 responses were used in the statistical analysis. We quantified responses calculating
179 the mean evoked depolarization in a 12 ms window after pip onset (auditory only trials, A) or after the
180 last tectal stimulus in tectal-only (tectal only trials, T) and multisensory (tectal + auditory trials, M)
181 trials (Supp. Fig. 1A-B). We also measured the peak amplitude of the response, which in nearly all cases
182 occurred in the same time window. As peak amplitude analysis produced the same qualitative results,
183 only the mean area analysis is shown.
184 To characterize the multisensory integration, the responses to M stimuli were normalized to the T and
185 A components. In the field of multisensory integration, multisensory responses are typically
186 normalized to the maximum response of the unisensory (Meredith and Stein, 1983; Stanford and
187 Stein, 2007; Stein and Stanford, 2008), which we call Multisensory-Maximum Unimodal index
188 (MSI/Max):
189
190 $$MSI/Max = M \div \max(T, A)$$
191
192 The value of this index determines the net effect of the integration, with MSI/Max greater than 1
193 representing multisensory enhancement, MSI/Max lower than 1 representing multisensory inhibition,
194 and MSI/Max not significantly different than 1 suggesting absence of multisensory integration (Stein
195 and Stanford 2008). Additionally, to calculate the linearity of the multisensory integration performed
196 by the M-cell, we calculated the ratio between the multisensory response and the sum of the
197 unisensory responses, which we call Multisensory-Sum Unimodals index (MSI/Sum):
198
199 $$\mathrm{MSI/Sum} = M \div (T + A)$$
200
201 The value of this index determines the linearity of the integration, with $\mathrm{MSI/Sum}$ greater than 1
202 representing supralinear integration, $\mathrm{MSI/Sum}$ of 1 representing linear integration, and $\mathrm{MSI/Sum}$
203 lower than 1 representing sublinear integration (Stanford et al., 2005).
204 One of the principles that guide multisensory integration is the spatial coherence of the different cues
205 being integrated. If the perceived source localizations of two stimuli overlap, these stimuli are more
206 likely be integrated. Conversely, if the two stimuli arrive from spatially disparate sources the chances
207 of observing a multisensory integration will decrease (Meredith and Stein, 1996; Stein and Stanford,

2008). The geometrical configuration of the setup in our experiments determined that the loudspeaker used to produce acoustic stimuli was mounted to the right of the fish and electrical stimulation was applied to the left tectum (which normally receives visual signals from the right retina). Whenever possible, we performed recordings from both Mauthner cells to minimize the number of fish used in the study. To rule out the possibility of a systematic difference on the responses of either M-cell due to the spatial source of the stimuli, we compared the responses to tectal or auditory stimuli in sequential recordings of the right and left M-cells of the same fish. Figure Supplementary 1 shows representative trace examples for tectal (100 ms 60 Hz tectal train, Fig. Supp. 1A) and auditory (5 ms 200 Hz auditory pip, Fig. Supp. 1B) stimulation from the left (upper traces) or right (lower traces) M-cell of the same fish. The complex post-synaptic potentials were highly stereotypical in successive presentations of a T (or A) stimulus within and across cells. Analysis from pairs of tectal (Supp. Fig. 1C, N=9) and auditory (Supp. Fig. 1D, N=11) M-cell responses showed no statistical differences between ipsi- and contralateral stimulation (paired T-test, tectal: p=0.788; auditory: p=0.467). This confirms previous results indicating that in goldfish, tectal stimulation produces responses with similar latency and amplitude in both M-cells (Zottoli et al., 1987; Canfield, 2006). We therefore pooled data acquired from left or right M-cells for all following analysis.

To perform statistical analysis, we used R (version 4.0.2, www.r-project.org) and RStudio (version 1.1.456, www. rstudio. com). A significance level of α = 0.05 was used throughout the study. Effects of explanatory variables over response variables were assessed using Linear Models (binomial GLMs in the case of binary variables, Linear Models (LM, followed by ANOVA) in the case of continuous variables). Paired T-tests were used to compare tectal or auditory responses recorded in left or right M-cells (see Fig. Supp. 1). The Wilcoxon Ranked Sum test was used for single sample comparisons. Sample size is denoted by *N* when it refers to the number of M-cells or *n* when it refers to the number of trials (average of 5-10 presentations). Boxplots show the median, 25 and 75th percentile, and lines indicate minimum and maximum values.

235 RESULTS

236

237 **MAUTHNER CELL RESPONSES ARE SENSITIVE TO THE DYNAMICS OF VISUAL TECTAL STIMULI**

238 Multisensory integration is known to be dependent on the saliency of the unimodal components
239 (Stanford et al., 2005; Martorell and Medan, 2022). To create a stimulus set of variable strength and
240 temporal dynamics, we recorded M-cell responses to different electrical trains delivered in the optic
241 tectum. The tectal stimuli we used produced M-cell responses that are reminiscent of those caused
242 by looming stimuli that simulate the approach of an object (Preuss et al., 2006; Medan and Preuss,
243 2014). Because responses to visual looms are significantly affected by repeated stimulation and
244 anesthesia, we chose tectal trains that evoke stable responses for the duration of the experiments.

245 M-cells respond to tectal trains of electrical stimulation with phasic postsynaptic potentials riding on
246 top of a tonic depolarizing response (Figure 1A) that reaches a plateau after 30-100 ms and decays to
247 resting values 200-300 ms after the end of the tectal train. To characterize how the M-cell responses
248 depend on the frequency and duration of the stimulation trains in the optical tectum, we recorded
249 responses to 60-Hz trains that varied in duration (Figure 1A-B), and 100-ms tectal trains that varied in
250 pulse frequency (Figure 1C-D). The responses to both sets of trains exhibited complex temporal
251 dynamics with a tonic component that progressively builds during the train and a fast phasic
252 component after each pulse (Figure 1A').

253 Increasing the duration of the 60-Hz trains drove stronger tectal responses due to the increase of the
254 tonic component of the response while the phasic response remained unchanged (ANOVA, tonic
255 $p<0.0001$, phasic $p= 0.63$, Figure 1A, B). Increasing the frequency of the 100-ms stimulation trains also
256 drove stronger tectal responses due to a large increase in the tonic component (ANOVA, tonic
257 $p<0.0001$). However, increasing the tectal stimulus frequency produced a significant reduction in the
258 amplitude of the phasic component (ANOVA, tonic $p<0.0001$, Figure 1C, D). Comparing the stimulus
259 trains of variable duration and frequency reveals that modifying the duration of the 60-Hz trains or
260 the frequency of 100-ms trains is similarly effective in tuning the magnitude of the responses.
261 Increasing the duration of a 60 Hz from 33 to 200 ms produced a 45% increase in the total response
262 amplitude (phasic + tonic) while increasing the frequency from 30 to 200 Hz produced a 50% increase
263 in the response amplitude (Figures 1 B, D). Since multimodal integration is known to depend on the
264 strength of the unimodal components (Stanford et al., 2005; Martorell and Medan, 2022), in the
265 following multimodal experiments we leveraged this characterization to generate tectal stimuli of
266 variable strength and dynamics. Although both the 60-Hz trains of variable duration and the 100-ms
267 trains of variable frequency evoked responses of similar total amplitude, we decided to include both

268 the sets of trains in our multisensory stimuli to determine whether any detected effect depended on
269 the temporal structure of the stimulus or the ratio of phasic-to-tonic responses.

270 **MULTISENSORY ENHANCEMENT IN THE MAUTHNER CELL**

271 Although the M-cell is known to respond to stimuli of different modalities, there are no reports on
272 how it combines and integrates information when two stimuli of different modalities are co-
273 presented. To determine whether multisensory enhancement occurs in the M-cell, we recorded
274 somatic responses to an auditory pip (unisensory auditory, A), a tectal stimulation train (unisensory
275 tectal, T), and their combination (multisensory audiotectal, M) (Figure 2A, E).
276 Increasing the duration of the 60-Hz tectal train positively modulated the multisensory responses
277 (amplitudes ranging from 3.10 ± 0.95 mV to 5.43 ± 1.80 mV, N = 17, n =74; LM: evoked depolarization
278 ~ tectal duration, $p<0.001$, Figure 2B). We then compared the multisensory responses to their
279 unisensory counterparts. When M responses were normalized to the most effective unisensory
280 response, multisensory stimuli yielded MSI/Max indices that ranged from 1.43 to 1.54 for all stimulus
281 durations (Wilcoxon single sample test mu=1, $p<0.001$ for all stimulus durations, Figure 2C), indicating
282 a significant multisensory enhancement of the response. When the M response was normalized to the
283 sum of both unisensory responses the MSI/Sum indices were lower than 1 (i.e. sublinear integration,
284 Wilcoxon single sample test mu=1, alternative mu<1, $p<0.001$) for all cases except for the briefest
285 tectal stimulus, for which the multisensory integration was supralinear (Wilcoxon single sample test
286 mu=1, alternative mu>1, $p<0.01$, Figure 2D).
287 Increasing the frequency of a 100-ms tectal train (Figure 2E) was not as effective in modulating the
288 multisensory responses (LM: evoked depolarization ~ tectal frequency, $p=0.07$, Figure 2F). However,
289 the M responses still exhibited MSI/Max indices that ranged 1.44-1.53 when compared to the largest
290 unimodal stimulus (Figure 2G) indicating that a 100 ms tectal train (irrespective of its frequency)
291 significantly enhances the M-cell response. The MSI/Sum of these M responses ranged 0.82 to 0.86
292 showing a similar sublinear integration to that of the multisensory stimuli with the longer 60-Hz trains
293 (Wilcoxon single sample test mu=1, alternative mu<1, all $p<0.001$, Figure 2H). Neither MSI/Max or
294 MSI/Sum showed a significant dependency with tectal frequency (LM: MSI/Max ~ tectal frequency,
295 $p=0.98$, MSI/Sum ~ tectal frequency, $p=0.27$).
296 Overall, these results show that, in all cases, combining an auditory pip with a preceding tectal pulse
297 enhances the M-cell response by about 50%. This multisensory enhancement does not show a strong
298 modulation by the duration or frequency of the tectal stimulus (Figure 2C, G). Noteworthy, while most
299 multisensory stimuli exhibited a sublinear integration, the multisensory stimulus with the shortest
300 (and weakest) tectal component produced a slightly but significantly supralinear response.
301

302 **TECTAL AND AUDITORY-EVOKED FEEDFORWARD INHIBITIONS EXHIBIT DISTINCT TEMPORAL**
303 **DYNAMICS**
304
305 Both visual and auditory stimuli evoke feedforward inhibition (FFI) at the perisomatic region of the M-
306 cell through a population of inhibitory interneurons which open chloride channels that produce
307 shunting of the postsynaptic currents (Diamond et al., 1973; Zottoli et al., 1987; Koyama et al., 2011;
308 Tabor et al., 2018). The functional roles of FFI include restricting the temporal window of sensory
309 excitation to terminate the excitatory signal. In combination with passive membrane decay, an
310 increase in FFI will further narrow the window for temporal integration. Conversely, a decrease in FFI
311 would increase lingering of a membrane depolarization produced by a previous stimulus, and thus
312 extend the temporal integration window. Thus differences in the strength or temporal dynamics
313 between visual and auditory evoked FFI may affect multisensory integration (Felch et al., 2016). In the
314 M-cell, auditory or tectal evoked FFI can be quantified as the amplitude reduction of an antidromically
315 evoked "test" action potential (APtest) (Faber and Korn, 1982, Medan et al. 2017). We used a single
316 auditory pip and a brief tectal train as "conditioning" stimuli of similar strength, which evoked
317 comparable depolarizations in the M-cell (~5 mV). To test if FFI evoked by auditory or tectal stimuli
318 differed, we evoked the APtest at specific times (2–80 ms) following a sensory stimulus and calculated
319 shunting inhibition as %SI= 100 - APtest/APcontrol ×100, where AP control is the amplitude of the AP
320 without a conditioning stimulus (Figure 3A). FFI inhibition induced by auditory and tectal stimulation
321 showed similar maximum amplitude (Figure 3B, auditory vs. tectal %SI: 13.65 ± 4.74 vs. 14.55 ± 7.50;
322 Kruskal-Wallis chi-squared = 0.01, p = 0.91) with peak inhibition at the same time (auditory vs. tectal
323 time (ms) of maximum %SI: 9.04 ± 3.93 vs. 8.85 ± 6.54; Kruskal-Wallis chi-squared = 0.30, p = 0.58,
324 Figure 3C). In a subset of experiments (N = 7), both auditory and tectal FFI were evaluated sequentially
325 in the same cell and same recording site which allowed us to have an accurate estimate of the
326 inhibition triggered by each sensory modality (Figure 3D). Although the maximum level of inhibition
327 was comparable and was reached in a similar time, recovery from inhibition was much faster for tectal
328 than for auditory FFI. Tectal FFI decayed to 50% of its peak in 8 ms, compared to 30 ms for the auditory
329 FFI (Kruskal-Wallis chi-squared = 5.97, p = 0.01, Figure 3E). In addition, the area under the curve for
330 auditory FFI was almost 3 times greater than for tectal FFI (502 vs. 176 %.ms, respectively, Kruskal-
331 Wallis chi-squared = 5.59, p = 0.02, Figure 3F).
332 These results highlight the key role of the temporal dynamics of the inhibition that reaches the M-cell
333 and which in turn will affect integration in the M-cell. Moreover, these results show that brief auditory
334 stimuli trigger more prolonged inhibition than similarly brief tectal stimuli. The short-lived FFI that
335 follows tectal stimulation suggests that multiple trains or waves of tectal inputs are more likely to be

integrated and summed than multiple sounds. This goes in line with duration of visual looms that are most effective in triggering the M-cell and eliciting visual C-start escapes (Preuss et al., 2006; Temizer et al., 2015). Differences on the decay rate of inhibition produced by brief tectal or auditory stimuli could affect integration of pairs of brief sensory stimuli depending on their sequence and their timing, which is explored in the next section.

STIMULUS TEMPORAL ORDER AND MODALITY AFFECT STIMULI INTEGRATION

There are several anatomical and functional differences in the pathways followed by auditory and visual inputs that eventually reach the M-cell soma. First, auditory inputs reach the lateral dendrite of the M-cell through a disynaptic (≈2 ms) pathway, while visual inputs reach the ventral dendrite after a polysynaptic (≈20 ms) pathway that includes the optical tectum (Zottoli et al., 1987; Szabo et al., 2006). Second, M-cell dendritic characteristics determine modality specific filtering differences resulting in stronger attenuation of visual than auditory signals (Medan et al., 2017). For auditory stimuli, it has been reported that a first sound reduces the M-cell response to a second sound, a phenomenon known as auditory prepulse inhibition (Neumeister et al., 2008; Curtin and Preuss, 2015; Tabor et al., 2018). However, it is unclear whether a similar phenomenon would hold true for cross-modal and tectal-tectal interactions, since auditory and visual inputs travel through distinct and separated pathways and undergo different filtering.

To investigate the role of input modality on M-cell integration we used pairs of similarly brief (~10 ms) auditory pips and tectal pulses 50 ms apart with in all possible sequences, including unisensory combinations: AT, TA, AA and TT (Figure 4A). The amplitude of the tectal stimulation pulse was chosen so that the M-cell responses to the tectal and auditory stimuli were of similar magnitude (4-8 mV). These initial responses decayed passively over the course of the 50 ms following the presentation of the first stimulus. The mean lingering depolarization from the evoked auditory pip in the AA and AT trials (shaded rectangles in Figure 4A) was larger than for the tectal stimulus in the TA and TT trials (1.12 ± 0.56mV vs. 0.75 ± 0.36mV, t-test: $p=0.03$, Figure 4B). This is consistent with previous results showing that visual (tectal) input is subject to stronger decay than auditory inputs (Medan et al., 2017). The response to the second stimulus was calculated using the voltage immediately before its presentation as baseline, which also represented the lingering depolarization. In the AA trials, we observed the previously described prepulse inhibition phenomenon, with the first auditory pip reducing the amplitude of the second pip by 40% (Neumeister et al., 2008; Curtin and Preuss, 2015; Tabor et al., 2018). To quantify the effect of the first stimulus on the second stimulus and compare the effect of its modality, we calculated the ratio between the amplitude of the second stimulus (A or

370 T) and the lingering depolarization plus its amplitude without a preceding stimulus (i.e. in a
371 "unisensory condition"). Note that this is the same quantitative analysis as in MSI/Sum with the
372 exception that one of the unisensory components is the lingering depolarization from the first stimulus
373 and that not all sequences are multisensory (i.e., AA and TT). Notably, the inhibitory effect observed
374 in the AA trials was not present for the other cross-modal and tectal-tectal combinations, with all of
375 them showing no reduction in the amplitude of the response to the second stimulus (Figure 4C, LM,
376 $F=72.7$, $p<0.001$).
377
378 **MULTISENSORY INTEGRATION IN THE MAUTHNER CELL SHOWS INVERSE EFFECTIVENESS**
379
380 The principle of inverse effectiveness states that the effects of multisensory integration are typically
381 larger when the components of a multisensory stimulus are weak. Throughout our experiments, we
382 observed that the M-cell only integrated supralinearly when presenting M stimuli with single tectal
383 pulse (Figure 2C, 1ms tectal), linearly when presenting brief (~10 ms) trains (Figure 4, AT – TA), and
384 sublinearly for M stimuli with longer tectal trains (Figure 2D-H). However, these results represent the
385 average MSI for each group for a specific set of experimental conditions and effectively simplify the
386 diverse range of responses across trials, experimental conditions, and fish. To compare the overall
387 dependence of the multisensory enhancement on the strength of sensory inputs, we pooled the
388 multisensory integration indexes for all fish and for all experiments irrespective of sequence of stimuli,
389 tectal duration and frequency (Figure 5A, MSI/Max and B, MSI/Sum). We found a significant inverse
390 correlation between the magnitude of the multisensory enhancement and the magnitude of the
391 unisensory components (LM: MSI/Max, $p<0.001$; MSI/Sum, $p<0.001$). This result parallels the inverse
392 effectiveness reported at the behavioral level in goldfish (McIntyre and Preuss, 2019; Martorell and
393 Medan, 2022), confirming that the relative multisensory enhancement obtained by combining two
394 inputs is proportionally higher when the stimuli are weak. Combinations of weak stimuli produce
395 supralinear multisensory responses that are between 50-100% stronger than the most effective
396 unisensory stimulus (Figure 5A). Noteworthy, these results provide robust evidence that in the escape
397 network of fish, inverse effectiveness of multisensory integration is implemented, at least, at the single
398 (Mauthner) cell level.
399 Although our analysis was based on subthreshold responses, in some cases we observed that the
400 multisensory enhancement of the response was sufficient for surpassing the threshold and generated
401 action potentials in the M-cell. Figure 5C shows two examples from two different animals in which the
402 M-cells showed subthreshold responses to unisensory stimuli and elicited an action potential when
403 the two stimuli are combined. Since an action potential in the M-cell triggers the initiation of a C-start

404 escape, these are examples of behaviors that only occurred in response to a multisensory stimulus but
405 not to either of the unisensory components. We did not see any action potential in response to
406 unisensory stimuli across 18 animals. This highlights how, because of the all-or-nothing nature of
407 action potentials, relatively small increments in the M-cell response due to multisensory enhancement
408 could be sufficient to make the cell trigger and have a profound effect in escape behavior, even if the
409 integration is sublinear.
410

411 DISCUSSION

412 The Mauthner-cell system triggers a behavior of vital importance: escaping from predators. A
413 combination of fast afferent circuits, synaptic specialization, special intrinsic properties and topology
414 of the M-cell contribute in concert to a fast startle escape response (Korn and Faber, 2005, Eaton et
415 al. review). Here we show that the M-cell incorporates multisensory information to enhance its
416 responses and characterize how the integration of multiple stimuli is affected by the modality, spatial
417 source, temporal structure, temporal order, and intensity of the stimuli. Although multisensory
418 enhancement has been previously described in different neural populations and across a wide range
419 of species, it was unclear whether the activity of these neurons was necessary, sufficient, or even
420 influenced the execution of behavioral responses to multisensory stimuli. In contrast to other known
421 multisensory structures of vertebrates multisensory integration in the M-cell has an unequivocal
422 function in fish behavior and survival, as it directly determines whether and when a C-start is triggered
423 (McIntyre and Preuss, 2019; Martorell and Medan, 2022) .

424 Different factors differentially affect the summation and integration of auditory and visual inputs to
425 the M-cell. First, sensory inputs are subject to different decays depending on the site of the dendritic
426 arbor at which they arrive. Auditory inputs reach the M-cell lateral dendrite through dense mixed
427 electrical and chemical synapses driven through the eighth nerve afferents (Szabo et al., 2006). In
428 contrast, visual inputs arriving to the ventral dendrite establish synapses that do not show additional
429 specializations as the club endings (Zottoli et al., 1987; Cachope et al., 2007; Szabo et al., 2007).
430 Second, the geometrical properties of the M-cell lateral and ventral dendrites (length and tapering)
431 impose different filters on the input signal which determine a stronger spatial decay for visual than
432 for auditory signals (Medan et al., 2017). Third, as excitatory signals reach the soma, the active ion
433 conductances decrease the membrane resistance and impact the response to following signals
434 (Hodgkin, 1947).

435 These factors modulate the effective multisensory integration in the M-cell soma, which emerges as
436 a complex, nonlinear interaction between “positive” (input strength and summation) and “negative”
437 (temporal and spatial decay, feedforward inhibition and depolarization-induced decrease in input
438 resistance) contributions. Although these factors likely influence integration in any sensory neuron,
439 the accumulated knowledge on the presynaptic pathways and the intrinsic mechanisms operating in
440 the M-cell combined with its functional role in commanding the initiation of the C-start response
441 makes this neuron a unique model for analyzing multisensory integration in a single identifiable
442 neuron.

443 We have previously shown that fish exhibit a behavioral multisensory enhancement of the C-start
444 escape response for audiovisual stimuli, and that this effect is reduced when salience of the unisensory

445 stimuli increases (Martorell and Medan, 2022). Therefore, one of our goals here was to investigate if
446 the inverse effectiveness principle observed behaviorally had its correlate in integration processes
447 taking place in the M-cell. Paralleling our previous behavioral results, here we show through
448 intracellular recordings that the response evoked by an auditory pip can be increased by about 50%
449 when it is preceded by a tectal stimulus (Figure 2C, G). This enhancement was not modulated by
450 relatively large changes in stimulus frequency. The plateau in the tonic depolarization observed 30-50
451 ms after a sustained stimulus (Figure 1A) combined with the low-pass filtering properties of the
452 membrane could be responsible for the lack of frequency effects. These two mechanisms point to the
453 M-cell role as a "sudden" stimulus detector rather than a precise coder of sensory stimulus properties.
454 When we combined a tectal train with an auditory pip to obtain a multisensory stimulus, the response
455 was smaller than the sum of the evoked depolarization of the two components (Figures 2D, H). This
456 sublinear integration was expected, since cellular biophysics predict a sublinear integration of
457 subthreshold inputs due to a reduction in the driving force of sodium and the aperture of ion channels
458 that reduce the membrane resistance. Noteworthy, action potentials are all-or-nothing events, so the
459 effects when the membrane potential is close to the threshold, sublinear summation can determine
460 that an otherwise silent neuron fires an AP (Figure 5C). Therefore, a weak (subthreshold) auditory pip
461 combined by a weak visual stimulus in close temporal association might be sufficient for triggering an
462 escape response.
463 Importantly, for the weakest multisensory stimuli the M-cell response deviated from this sublinear
464 integration (Figures 2C and 5A). When the sum of unisensory components is less than 2.5 mV
465 (essentially a single tectal stimulus immediately followed by a single auditory pip) summation is
466 supralinear (Figure 2D and 5A). This suggests the existence of one or more active (supralinear)
467 mechanism/s of multisensory integration upstream of the M-cell soma, potentially through a
468 presynaptic neuron that also receives audiovisual inputs and projects to the M-cell or locally at the
469 level of the dendritic tree of the M-cell. Indeed, modelling experiments have suggested that active
470 conductances expressed in the proximal dendrites of the M-cell confer nonlinear properties to the
471 lateral and ventral dendrites that increases their excitability. This in turn could particularly enhance
472 multisensory integration of weak stimuli (Medan et al., 2017) providing a cellular mechanism for the
473 principle of inverse effectiveness of multisensory integration.
474 The temporal structure of the multisensory stimuli is crucial to allow the animal to effectively "bind"
475 or associate both signals as coming from a single source (Stein and Stanford, 2008). In the M-cell, this
476 translates into the time window where the effect on the membrane voltage (excitatory and/or
477 inhibitory) persists. Here, we found that a delay of 50 ms between the components of a low-amplitude
478 multisensory stimuli result in a linear summation of the signals (Figure 4C) and that the temporal order

of the components does not affect the integration (Figure 4C, AT vs. TA) (Felch et al., 2016). On the other hand, the integration of unisensory stimuli was dependent on the modality of the stimuli: two tectal (TT) stimuli summed linearly while two auditory (AA) stimuli summed sublinearly (Figure 4C). This difference is probably due to differences in both the presynaptic networks that mediate PPI (Tabor et al., 2018) and in the temporal decay of auditory and tectally evoked FFI (Figure 3D). Auditory stimuli produce not only a longer-lasting inhibition than tectal stimuli of similar strength, but also generate a slow-decaying depolarization upon which the tectal stimulus can sum (Figure 4B). While tectal inhibition is almost extinct 50 ms after a tectal stimulus, auditory inhibition stabilizes at around 50% of the maximum inhibitory effect in a time window of 30 to 70 ms after an auditory stimulus (Figure 3E). Interestingly, the integration of AT stimuli was similar to that of TA, supporting a differential cross-modal and intra-modal integration of the excitatory or inhibitory components. Another factor that could be contributing to the differential integration between AA and AT stimuli is that FFI inhibition is likely to be heterogeneously spread in the perisomatic area around the M-cell. If auditory stimulation recruits inhibitory PHP neurons that target the proximal lateral dendrite of the M-cell, a subsequent sensory input propagating along the lateral dendrite (i.e, auditory input) would suffer stronger attenuation than one reaching the soma through the ventral dendrite (i.e., tectal input). However, specific studies are required to test this hypothesis as it is still unclear if auditory and tectal afferent fibers contact the same or different sets of inhibitory neurons and which is the spatial distribution of those inhibitory contacts. Additionally, presynaptic effects could also contribute to the asymmetry in unimodal auditory (AA) vs. unimodal tectal (TT) or multisensory processing. A subset of glutamatergic Gsx1 neurons located in rhombomere 4 have been shown to mediate M-cell auditory presynaptic inhibition (Tabor et al., 2018). These neurons produce presynaptic inhibition of 8th nerve auditory fibers adjacent to the distal portion of the M-cell lateral dendrite but leave unaffected the ventral dendrite. This mechanism could therefore affect the processing of pairs of auditory signals (AA) and leave the integration of tectal or multisensory stimuli unaffected.

AUTHOR CONTRIBUTIONS

SOC, TP and VM conceived the research. SOC and VM performed experiments and analyzed the data. SOC, TP and VM wrote the manuscript.

512 **References**

513 Cachope R, Mackie K, Triller A, O'Brien J, Pereda AE (2007) Potentiation of electrical and chemical
514 synaptic transmission mediated by endocannabinoids. Neuron 56:1034–1047.

515 Canfield JG (2006) Functional evidence for visuospatial coding in the Mauthner neuron. Brain Behav
516 Evol 67:188–202.

517 Cordova MS, Braun CB (2007) The use of anesthesia during evoked potential audiometry in goldfish
518 (Carassius auratus). Brain Res 1153:78–83.

519 Curtin PCP, Preuss T (2015) Glycine and GABAA receptors mediate tonic and phasic inhibitory
520 processes that contribute to prepulse inhibition in the goldfish startle network. Front Neural Circuits
521 9:12.

522 Dean P, Redgrave P, Westby GWM (1989) Event or emergency? Two response systems in the
523 mammalian superior colliculus. Trends Neurosci 12:137–147.

524 Diamond J, Roper S, Yasargil GM (1973) The membrane effects, and sensitivity to strychnine, of
525 neural inhibition of the Mauthner cell, and its inhibition by glycine and GABA. J Physiol 232:87–111.

526 Faber DS, Korn H (1982) Transmission at a central inhibitory synapse. I. Magnitude of unitary
527 postsynaptic conductance change and kinetics of channel activation. J Neurophysiol 48:654–678.

528 Faber DS, Korn H (1989) Electrical field effects: their relevance in central neural networks. Physiol
529 Rev 69:821–863.

530 Felch DL, Khakhalin AS, Aizenman CD (2016) Multisensory integration in the developing tectum is
531 constrained by the balance of excitation and inhibition. eLife 5:e15600.

532 Furshpan EJ, Furukawa T (1962) Intracellular and extracellular responses of the several regions of the
533 Mauthner cell of the goldfish. J Neurophysiol 25:732–771.

534 Furukawa T (1966) Synaptic Interaction at the Mauthner Cell of Goldfish. In: Progress in Brain
535 Research (Tokizane T, Schadé JP, eds), pp 44–70 Correlative Neurosciences. Elsevier. Available at:
536 https://www.sciencedirect.com/science/article/pii/S0079612308629714 [Accessed October 24,
537 2022].

538 Hodgkin AL (1947) The membrane resistance of a non-medullated nerve fibre. J Physiol 106:305–
539 318.

540 Kadunce DC, Vaughan JW, Wallace MT, Stein BE (2001) The influence of visual and auditory receptive
541 field organization on multisensory integration in the superior colliculus. Exp Brain Res 139:303–310.

542 Korn H, Faber DS (2005) The Mauthner cell half a century later: a neurobiological model for decision-
543 making? Neuron 47:13–28.

544 Koyama M, Kinkhabwala A, Satou C, Higashijima S, Fetcho J (2011) Mapping a sensory-motor
545 network onto a structural and functional ground plan in the hindbrain. Proc Natl Acad Sci U S A
546 108:1170–1175.

547 Martorell N, Medan V (2021) Audiovisual integration in the Mauthner cell enhances escape
548 probability and reduces response latency. Available at:
549 https://www.biorxiv.org/content/10.1101/2021.08.19.456957v1 [Accessed August 27, 2021].

550 Martorell N, Medan V (2022) Audiovisual integration in the Mauthner cell enhances escape
551 probability and reduces response latency. Sci Rep 12:1097.

552 McIntyre C, Preuss T (2019) Influence of Stimulus Intensity on Multimodal Integration in the Startle
553 Escape System of Goldfish. Front Neural Circuits 13:7.

554 Medan V, Mäki-Marttunen T, Sztarker J, Preuss T (2017) Differential processing in modality-specific
555 Mauthner cell dendrites. J Physiol.

556 Medan V, Preuss T (2014) The Mauthner-cell circuit of fish as a model system for startle plasticity. J
557 Physiol-Paris 108:129–140.

558 Meredith MA, Stein BE (1983) Interactions among converging sensory inputs in the superior
559 colliculus. Science 221:389–391.

560 Meredith MA, Stein BE (1996) Spatial determinants of multisensory integration in cat superior
561 colliculus neurons. J Neurophysiol 75:1843–1857.

562 Neumeister H, Szabo TM, Preuss T (2008) Behavioral and physiological characterization of
563 sensorimotor gating in the goldfish startle response. J Neurophysiol 99:1493–1502.

564 Palmer LM, Mensinger AF (2004) Effect of the anesthetic tricaine (MS-222) on nerve activity in the
565 anterior lateral line of the oyster toadfish, Opsanus tau. J Neurophysiol 92:1034–1041.

566 Preuss T, Faber DS (2003) Central cellular mechanisms underlying temperature-dependent changes
567 in the goldfish startle-escape behavior. J Neurosci 23:5617–5626.

568 Preuss T, Osei-Bonsu PE, Weiss SA, Wang C, Faber DS (2006) Neural representation of object
569 approach in a decision-making motor circuit. J Neurosci Off J Soc Neurosci 26:3454–3464.

570 Stanford TR, Quessy S, Stein BE (2005) Evaluating the Operations Underlying Multisensory
571 Integration in the Cat Superior Colliculus. J Neurosci 25:6499–6508.

572 Stanford TR, Stein BE (2007) Superadditivity in multisensory integration: putting the computation in
573 context. Neuroreport 18:787–792.

574 Stein BE, Stanford TR (2008) Multisensory integration: current issues from the perspective of the
575 single neuron. Nat Rev Neurosci 9:255–266.

576 Szabo TM, McCormick CA, Faber DS (2007) Otolith endorgan input to the Mauthner neuron in the
577 goldfish. J Comp Neurol 505:511–525.

578 Szabo TM, Weiss SA, Faber DS, Preuss T (2006) Representation of auditory signals in the M-cell: role
579 of electrical synapses. J Neurophysiol 95:2617–2629.

580 Tabor KM, Smith TS, Brown M, Bergeron SA, Briggman KL, Burgess HA (2018) Presynaptic Inhibition
581 Selectively Gates Auditory Transmission to the Brainstem Startle Circuit. Curr Biol CB 28:2527-
582 2535.e8.

583 Temizer I, Donovan JC, Baier H, Semmelhack JL (2015) A Visual Pathway for Looming-Evoked Escape
584 in Larval Zebrafish. Curr Biol CB 25:1823–1834.

585 Wei P, Liu N, Zhang Z, Liu X, Tang Y, He X, Wu B, Zhou Z, Liu Y, Li J, Zhang Y, Zhou X, Xu L, Chen L, Bi G,
586 Hu X, Xu F, Wang L (2015) Processing of visually evoked innate fear by a non-canonical thalamic
587 pathway. Nat Commun 6:6756.

588 Weiss SA, Zottoli SJ, Do SC, Faber DS, Preuss T (2006) Correlation of C-start behaviors with neural
589 activity recorded from the hindbrain in free-swimming goldfish (Carassius auratus). J Exp Biol
590 209:4788–4801.

591 Zottoli SJ (1977) Correlation of the startle reflex and Mauthner cell auditory responses in
592 unrestrained goldfish. J Exp Biol 66:243–254.

593 Zottoli SJ, Hordes AR, Faber DS (1987) Localization of optic tectal input to the ventral dendrite of the
594 goldfish Mauthner cell. Brain Res 401:113–121.

595

596

597 FIGURE LEGENDS

598 **Supplementary Figure 1**. A-B. Representative recordings of left or right M-cell somatic responses to
599 an electric stimulus train delivered to the left tectum (A) or to a short 200 Hz sound pip produced by
600 a loudspeaker placed to the right side of the fish (B). The mean (of 3-5 repetitions) response is shown
601 in solid color and either the diagram of the tectal stimulus or the microphone recording of the sound
602 pip are shown below the traces. Dashed boxes indicate the 12-ms time windows following the stimulus
603 where the responses were quantified. C-D. Boxplots showing the median, upper and lower quartiles
604 and comparing the response to the same stimulus in the left or right M-cell in 10 fish for the tectal
605 stimulus (C) and 11 fish for the auditory stimulus (D). Markers with the same color in left and right
606 belong to pairs of M-cells of the same fish. No differences were found in the evoked response
607 amplitude between the left and right M-cells or for tectal or auditory stimuli.

608

609 **Figure 1**. M-cell responses to tectal stimulation. A. M-cell responses to a 60 Hz tectal train of 200 ms
610 were used to measure the evoked depolarization at 1, 33, 100 and 200 ms after stimulus onset during
611 a 12-ms time window (colored vertical boxes). A´, Lower inset. Dark grey and light grey areas in the
612 trace show amplitudes of the tonic and phasic components of the response, respectively. The
613 horizontal dotted line indicates the baseline for quantification of each component. B. Mean amplitude
614 (± SEM) of the phasic (shaded) and tonic (solid) components of tectal trains for the time windows
615 described in A. N=13-14. C. M-cell responses to a 100 ms tectal pulse train of 30, 60, 100 or 200 Hz
616 were recorded and quantified as in A, at the end of the pulse. D. Mean amplitude (± SEM) of the phasic
617 (shaded) and tonic (solid) components of 100-ms tectal trains of different frequency. N=10-12.

618

619 **Figure 2**. Multisensory integration in the M-cell. A. Diagram of stimulation (left) and response
620 examples (right). The response examples correspond to a single acoustic pulse (blue), to a tectal train
621 of 200 ms at 60 Hz (red), and to their multisensory combination (purple). B. Stacked bars comparing
622 mean (± SEM) depolarization evoked by tectal, auditory or multisensory stimuli with tectal stimulus
623 trains of indicated duration. N=14-23. C. Boxplots showing the ratios between the multisensory
624 responses and the maximum unisensory response (MSI/Max). D. Boxplots showing the ratios between
625 the multisensory responses and the sum of its unisensory components (MSI/Sum). E-H. As in A-D but
626 for 100 ms tectal trains of different frequencies (N= 14-23).

627

628 **Figure 3**. Auditory and tectal FFI have different decay dynamics. A. Diagram of auditory or tectal
629 evoked feedforward inhibition circuits (center), and the quantification of sensory evoked shunting
630 inhibition as a reduction of M-cell AP amplitude (auditory: blue, tectal: red; shaded area on top of

trace examples) to a control AP (black trace). B-C. Boxplots of peak inhibition and time of peak inhibition triggered by acoustic (N= 21) or tectal stimuli (N= 20). D. Mean (±SEM, N= 7) FFI triggered by tectal and auditory inputs measured in the same M-cells at different time points between 0 and 70 ms post-stimulus. E. Boxplot of the time elapsed to 50% decay of peak FFI for the auditory (left) and tectal (right) stimuli. *p=0.01. F. Area below the curve (0-70 ms) for the auditory (left) and tectal (right) stimuli. *p=0.02.

Figure 4. Effect of stimulus sequence and modality on M-cell integration. A. Representative responses of one M-cell to a sequence of acoustic and tectal stimuli, with schematics below each trace showing the modality (auditory: blue, tectal: red) and temporal order of the stimulation. The two stimuli were presented at a 50 ms interval. The shaded blue or red rectangles represent the time windows at which the lingering depolarization of the first responses were measured. B. Lingering depolarization after a single auditory pip or a short tectal train. *p=0.03 (N=29-13). C. Integration in the M-cell for pairs of uni- or multisensory stimuli with a 50 ms delay was calculated as the ratio between the amplitude of the response to the 2nd stimulus over the sum of the lingering depolarization from the response to the first stimulus plus the amplitude of the response to the 2nd stimulus without a preceding stimulus in the same cell (*p<0.001 N=8-29).

Figure 5. Multisensory integration of subthreshold unisensory stimuli. A. Pooled responses to different multisensory stimuli, irrespective of duration, frequency, or sequence of stimulation, plotted based on the sum of the responses to its unisensory components and the MSI/Sum index. B. Similar to D, but with the MSI/Max index instead. C. Example traces in which the integration of subthreshold unisensory tectal (T, red) and auditory (A, blue) stimuli evokes an M-cell AP (TA, purple). Responses to an auditory pip only triggered an action potential when they were preceded by four tectal pulses delivered at 333Hz (left) or a 200-ms tectal train at 60Hz (right).

Supplementary Figure 1

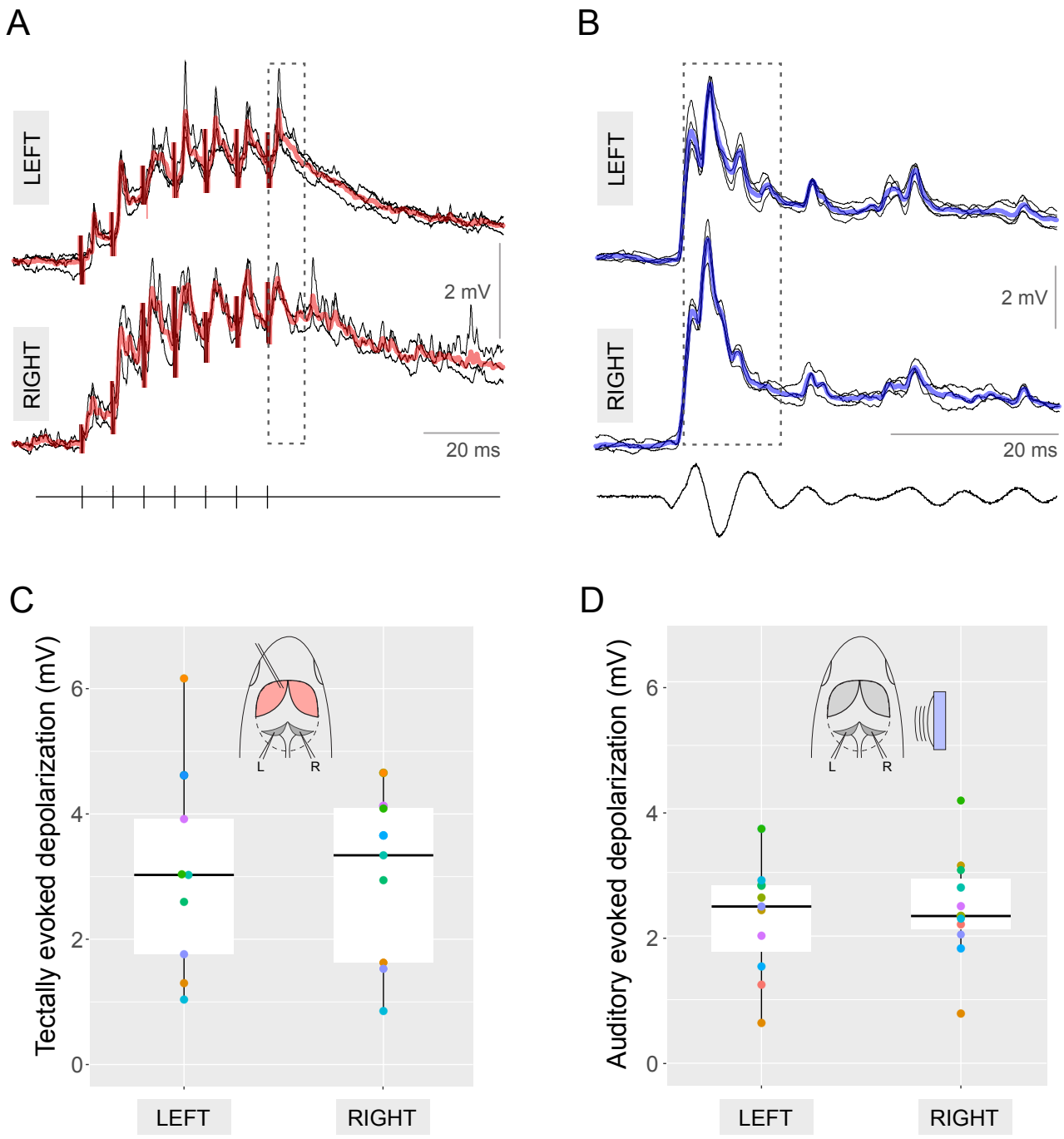

Figure 1

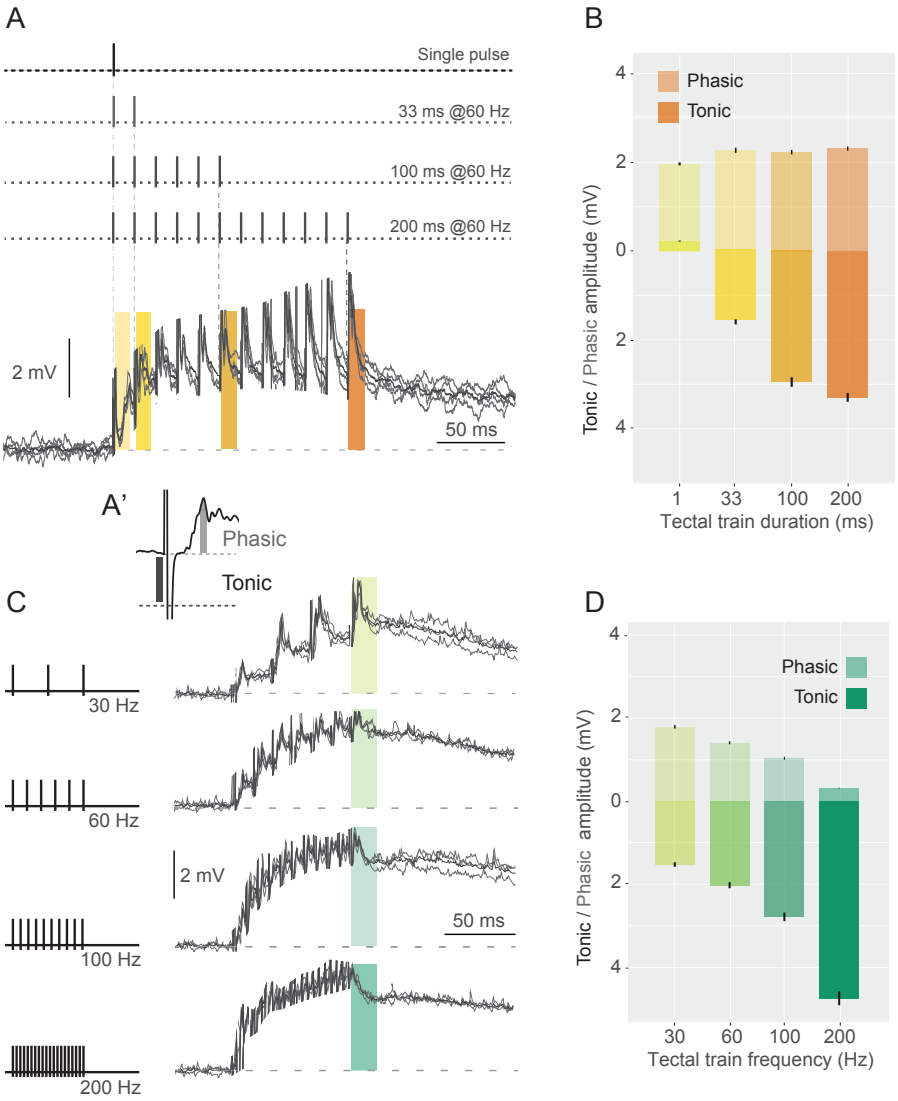
A
Single pulse
33 ms @60 Hz
100 ms @60 Hz
200 ms @60 Hz
2 mV
50 ms
A'
Phasic
Tonic
B
Phasic
Tonic
Tonic / Phasic amplitude (mV)
4
2
0
2
4
1
33
100
200
Tectal train duration (ms)
C
30 Hz
60 Hz
100 Hz
200 Hz
2 mV
50 ms
D
Phasic
Tonic
Tonic / Phasic amplitude (mV)
4
2
0
2
4
30
60
100
200
Tectal train frequency (Hz)

Figure 2

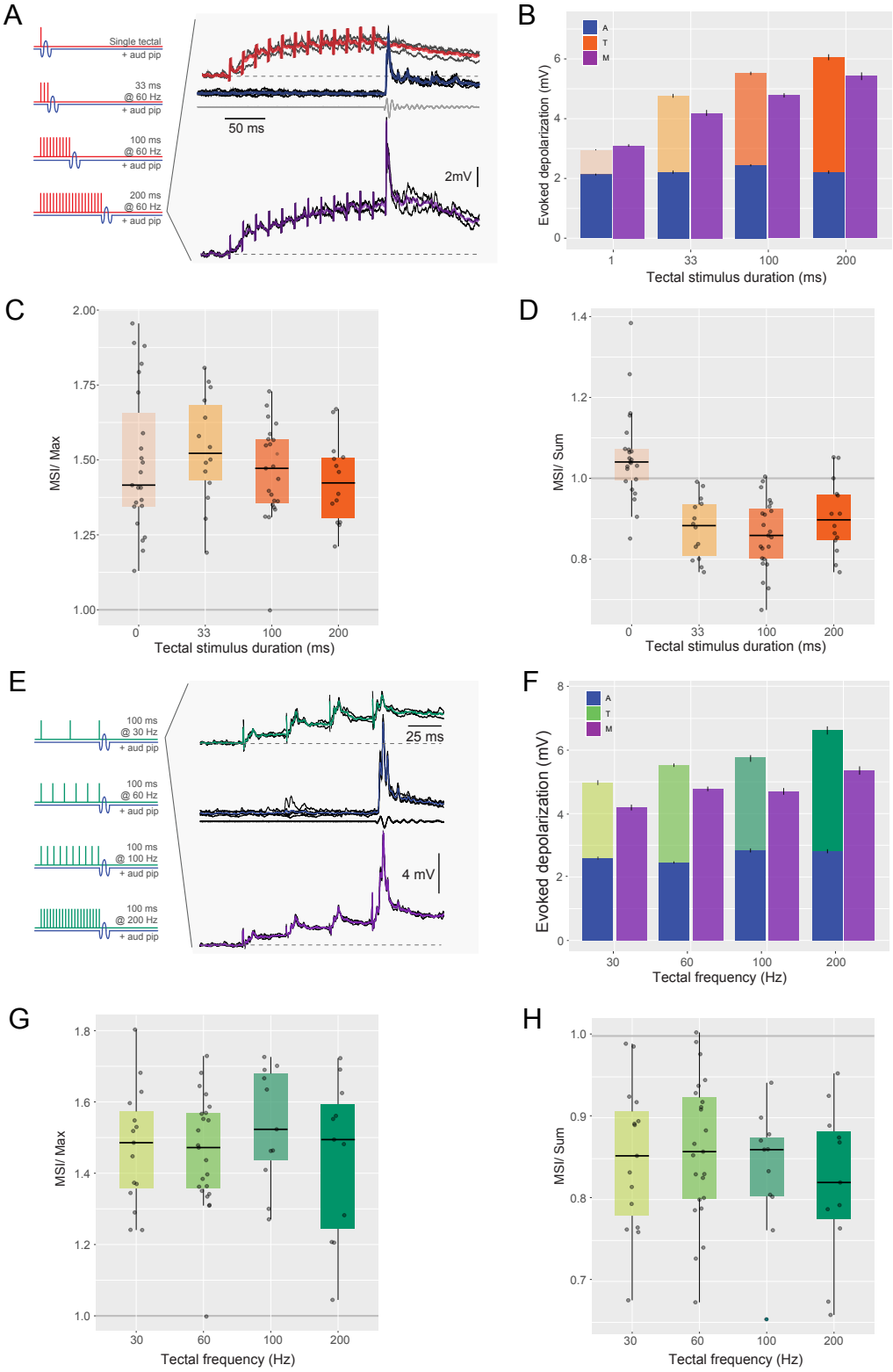
A
Single tectal
+ aud pip
33 ms
@ 60 Hz
+ aud pip
100 ms
@ 60 Hz
+ aud pip
200 ms
@ 60 Hz
+ aud pip
50 ms
2mV
B
A
T
M
Evoked depolarization (mV)
Tectal stimulus duration (ms)
C
MSI/ Max
Tectal stimulus duration (ms)
D
MSI/ Sum
Tectal stimulus duration (ms)
E
100 ms
@ 30 Hz
+ aud pip
100 ms
@ 60 Hz
+ aud pip
100 ms
@ 100 Hz
+ aud pip
100 ms
@ 200 Hz
+ aud pip
25 ms
4 mV
F
A
T
M
Evoked depolarization (mV)
Tectal frequency (Hz)
G
MSI/ Max
Tectal frequency (Hz)
H
MSI/ Sum
Tectal frequency (Hz)

Figure 3

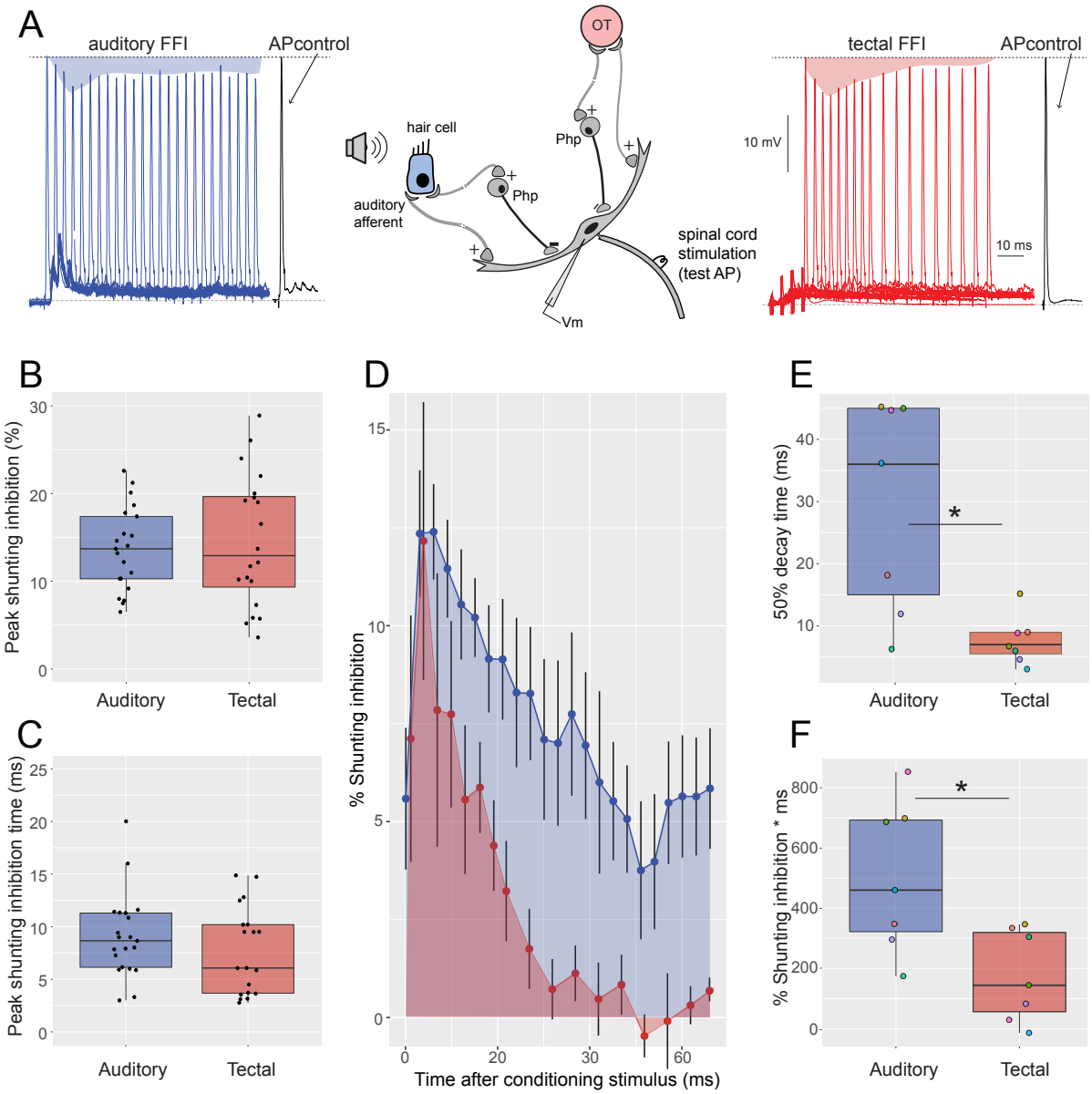
A
auditory FFI
APcontrol
hair cell
auditory afferent
Php
Php
OT
spinal cord stimulation (test AP)
Vm
tectal FFI
APcontrol
10 mV
10 ms
B
Peak shunting inhibition (%)
Auditory
Tectal
C
Peak shunting inhibition time (ms)
Auditory
Tectal
D
% Shunting inhibition
Time after conditioning stimulus (ms)
E
50% decay time (ms)
*
Auditory
Tectal
F
% Shunting inhibition * ms
*
Auditory
Tectal

Figure 4

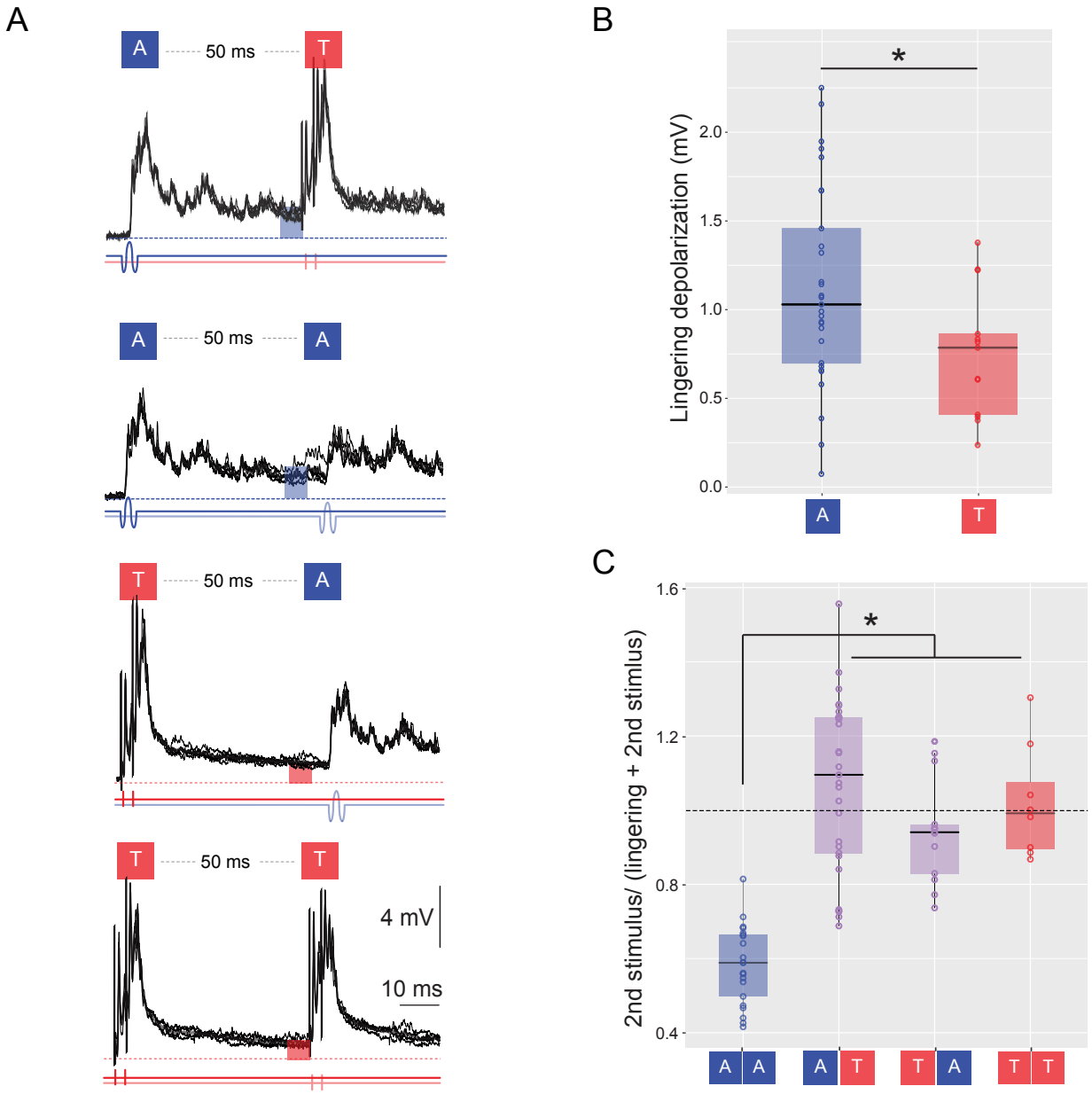
A
A
50 ms
T
A
50 ms
A
T
50 ms
A
T
50 ms
T
4 mV
10 ms
B
*
Lingering depolarization (mV)
2.0
1.5
1.0
0.5
0.0
A
T
C
*
2nd stimulus/ (lingering + 2nd stimlus)
1.6
1.2
0.8
0.4
A A
A T
T A
T T

Figure 5

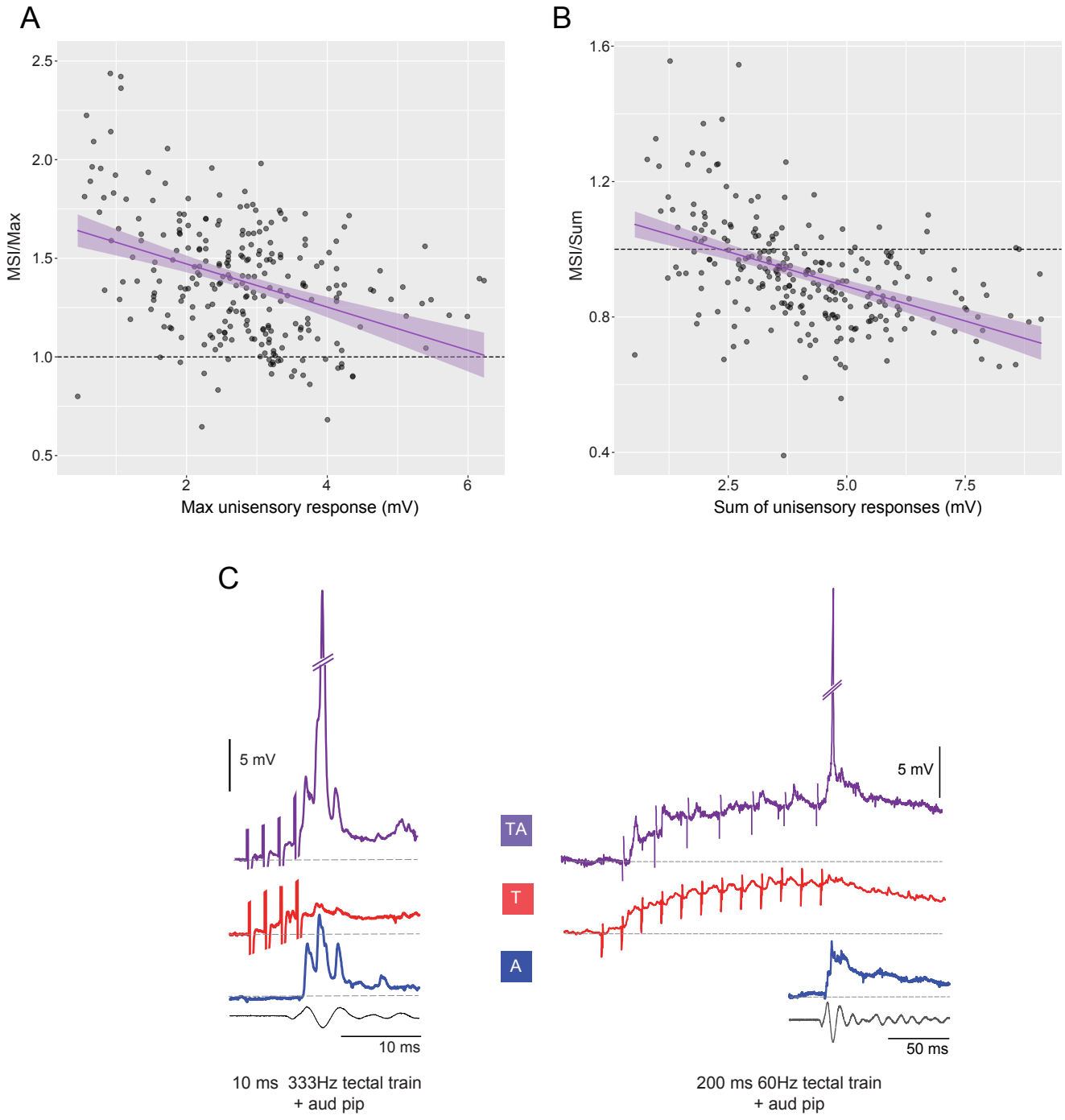
A
MSI/Max
2.5
2.0
1.5
1.0
0.5
2
4
6
Max unisensory response (mV)
B
MSI/Sum
1.6
1.2
0.8
0.4
2.5
5.0
7.5
Sum of unisensory responses (mV)
C
5 mV
10 ms
TA
T
A
5 mV
50 ms
10 ms 333Hz tectal train
+ aud pip
200 ms 60Hz tectal train
+ aud pip